Published in final edited form as:

Neuron. 2018 June 27; 98(6): 1133–1140.e3. doi:10.1016/j.neuron.2018.05.017.

Stable Sequential Activity Underlying the Maintenance of a Precisely Executed Skilled Behavior

Kalman A. Katlowitz[1,2], **Michel A. Picardo**[1,2], and **Michael A. Long**[1,2,3]

[1]NYU Neuroscience Institute and Department of Otolaryngology, New York University Langone Medical Center, New York, NY 10016 USA

[2]Center for Neural Science, New York University, New York, NY, 10003 USA

SUMMARY

A vast array of motor skills can be maintained throughout life. Do these behaviors require stability of individual neuron tuning or can the output of a given circuit remain constant despite fluctuations in single cells? This question is difficult to address due to the variability inherent in most motor actions studied in the laboratory. A notable exception, however, is the courtship song of the adult zebra finch, which is a learned, highly precise motor act mediated by orderly dynamics within premotor neurons of the forebrain. By longitudinally tracking the activity of excitatory projection neurons during singing using two-photon calcium imaging, we find that both the number and precise timing of song-related spiking events remain nearly identical over the span of several weeks to months. These findings demonstrate that learned, complex behaviors can be stabilized by maintaining precise and invariant tuning at the level of single neurons.

eTOC Blurb

By longitudinally tracking song-related activity in the zebra finch brain using two-photon imaging, Katlowitz et al. show that the timing of premotor sequences in a cortical region necessary for precise vocal production is maintained at the level of single neurons

Keywords

motor control; two-photon; calcium imaging; zebra finch; birdsong

*To whom correspondence should be addressed: Michael A. Long (mlong@med.nyu.edu).
[3]Lead contact

AUTHOR CONTRIBUTIONS

M.L. and M.P. designed the experiments. K.K. and M.L. wrote the paper. M.P. collected the data. K.K. analyzed the data with assistance from M.P. and M.L.

DECLARATIONS OF INTERESTS

The authors declare no competing interests.

INTRODUCTION

Following extensive training, skilled behaviors can often be executed with remarkable temporal precision (Glaze and Troyer, 2006; Hore and Watts, 2011; Kawai et al., 2015; Moore and Chen, 2010; Nasu et al., 2014; Wollner et al., 2012). However, considerable disagreement has emerged concerning the nature of the network activity in circuits underlying the production of these movements (Clopath et al., 2017; Lutcke et al., 2013). In one view, the *optimal manifold hypothesis* (Gallego et al., 2017; Rokni et al., 2007; Todorov and Jordan, 2002), a continuum of network configurations can produce a single desired behavior. In this scheme, individual neurons are often thought to be highly redundant (Narayanan et al., 2005; Takiyama and Okada, 2012) and capable of significantly changing their tuning over time, provided that the network itself remains constant (Carmena et al., 2005; Huber et al., 2012; Peters et al., 2017; Rokni et al., 2007). Others have proposed a *tuning constancy hypothesis* in which learned motor behaviors are the result of highly refined circuitry capable of producing reliable premotor commands across renditions (Chestek et al., 2011; Flint et al., 2016; Fraser and Schwartz, 2012; Ganguly and Carmena, 2009). To accomplish this, networks have to maintain their tuning over time at the level of individual neurons, potentially limiting robustness (Marder et al., 2015). A major obstacle preventing the characterization of network stability is the confound of variability in the behavior itself, which can occur as the result of motor noise (Chaisanguanthum et al., 2014; Churchland, 2015; Orban and Wolpert, 2011) or redundancies in the muscular patterns needed to achieve a specific task (Lashley, 1933; Latash, 2012), such the execution of a precise hand trajectory (Muceli et al., 2014).

To circumvent these potential sources of bias, we examined a complex behavior notable for its rigid stereotypy: song production in an adult zebra finch. After a significant learning phase consisting of ~10^5 repetitions (Tchernichovski et al., 2001), adult zebra finches flawlessly perform their song for the remainder of their lives (Immelmann, 1969; Lombardino and Nottebohm, 2000), with timing variability across renditions (song motifs) of less than 2% (Glaze and Troyer, 2006). Furthermore, because song relies on a small set of syringeal and respiratory muscles, only a specific combination of movements can achieve the correct singing behavior (Goller and Cooper, 2004). As a result, the songbird represents an ideal opportunity to examine the dynamics of premotor network patterns in the context of stable behavioral performance.

Song production in the zebra finch is dependent on the activity of dedicated brain areas, most notably the cortical premotor region HVC (proper name). During singing, approximately half of the HVC premotor neurons are active at different moments in the song (with the remainder silent during singing) (Hahnloser et al., 2002), forming a continuous sequence of activity (Lynch et al., 2016; Picardo et al., 2016) that generates vocal output (Long and Fee, 2008; Nottebohm et al., 1976; Vu et al., 1994). Electrophysiological studies have shown that each HVC projection neuron can reliably produce a high frequency burst of action potentials at a precise moment within the song with submillisecond precision across trials (Hahnloser et al., 2002; Kozhevnikov and Fee, 2007; Long et al., 2010). However, because such recordings are limited to a few hours in the best cases (Hahnloser et al., 2002; Vallentin and Long, 2015), these methods could not be used to assess the stability of the

network over longer periods of time. Recently, the activity of HVC projection neurons expressing the genetically encoded calcium indicator GCaMP6 was monitored longitudinally via a 1-photon head-mounted endoscope, demonstrating a high degree of variability in song-related activity over the span of five days (Liberti et al., 2016). Despite these apparent network changes, tracking individual neurons over time with the microendoscopic approach has been shown to be highly challenging, sometimes leading to errors in identifying individual neurons across sessions (Sheintuch et al., 2017; Zhou et al., 2018). To counteract this potential source of error, we used two-photon imaging in the songbird brain (Graber et al., 2013; Peh et al., 2015), which has the distinct advantage of optical sectioning (Denk et al., 1990), enabling us to monitor the activity of morphologically identified neurons over the span of several weeks in a recently developed head-fixed singing bird preparation (Picardo et al., 2016). Using this method, we measured the timing of premotor responses longitudinally over the span of several weeks and found that individual cells rarely changed their activity patterns, suggesting that a stable projection network is the source of the stability of the behavior and supporting the network constancy hypothesis. Our data provide a striking example of neural circuit reliability that may represent a general strategy for enabling other behaviors featuring precisely timed expert movements.

RESULTS

Long-term Imaging of Premotor Circuit Activity

To address whether song-related network dynamics were stable across days, we monitored the activity of GCaMP6-expressing HVC neurons during directed singing in 8 adult male zebra finches using two-photon calcium imaging (Figure 1). Three birds were newly imaged as part of this study, and data from an additional five birds were reanalyzed from our previous publication (Picardo et al., 2016). We imaged multiple sessions over an extended period of time, ranging from 8 to 60 days. Within individual birds, 339 neurons (9–68 per bird) fitting the profile of excitatory projection neurons (Hahnloser et al., 2002; Mooney, 2000; Picardo et al., 2016) were observed longitudinally over periods ranging from 2 to 57 days (Figure 1B), leading to a total of 1,618 daily observations (or ‘cell-days’) across all birds. Although we could not selectively express our activity indicator in a specific excitatory cell class, it is likely that we frequently sampled from both major projection cell types in this study. Specifically, the anatomical features of the imaged neurons (Dutar et al., 1998; Peh et al., 2015) are consistent with a mixture of two populations, one targeting the motor cortical structure known as the robust nucleus of the archipallium ($HVC_{(RA)}$) and one targeting the basal ganglia ($HVC_{(X)}$). For the remainder of the analysis presented here, we combine data from both groups.

The requirement to return to the same neurons across sessions is a challenge inherent in longitudinal imaging (Crowe and Ellis-Davies, 2014). Unlike single photon approaches, the exquisite spatial resolution afforded by two-photon microscopy enabled us to use morphological features to track individual neurons over time (Driscoll et al., 2017; Peters et al., 2014) (Figure 1C). To align imaging planes (approximately 500μm X 500μm), we applied a motion correction algorithm to align the averages of all trials and manually annotated single neurons on the average image from across days (see Methods). However,

the possibility existed that a portion of the imaging plane containing our neuron of interest was not consistent across days, as one might expect if the optical axis had shifted or a local aberration in the imaging pathway led to inconsistencies in the imaging plane. Such local warping could result in two possible sources of error, namely that the extracted fluorescence traces could simply reflect the absence of the neuron of interest or even the inclusion of a different neuron from a nearby plane. To address the former concern, we visually inspected the region of interest (ROI) for each cell-day, eliminating all cases in which the neuron was clearly outside of the focal plane, which comprised 5.6% of the total data set. To address the latter concern, we performed a two-dimensional spatial correlation on all the pixels within a 100 μm by 100 μm square field surrounding each neuron across all days (Figure 1C and 1D). We also performed the same analysis across other neurons with different local environments as a negative control, leading to the removal of only 0.4% of our final data set (Figure 1E, see Methods). Using smaller spatial scales (e.g., 50 μm by 50 μm) did not qualitatively change these results (~2% of the data rejected).

Song-Related Neural Activity is Stable Over Time

We next calculated the song-related timing for each of our longitudinally recorded neurons for individual days. Based on previous electrophysiological reports that bursts are robust and stable on the timescale of our experiment (~1 hour) (Hahnloser et al., 2002; Kozhevnikov and Fee, 2007; Long et al., 2010), we assumed that burst times that give rise to each fluorescence trace for a given neuron should be invariant within an imaging session. We used a Markov Chain-Monte Carlo approach, extending a continuous time Bayesian deconvolution algorithm to account for multiple trials (Picardo et al., 2016; Pnevmatikakis et al., 2016). We approximated the posterior distribution of these shared times, allowing us to define not only the location of burst onsets but also their associated uncertainty (see Methods). Typically, we acquired multiple song motifs within a session (6.5±4.9 motifs per cell-day) to sharpen the temporal resolution of our estimates of single neuron activity (Picardo et al., 2016; Pnevmatikakis et al., 2016). Using this approach, we were able to reliably extract precise onset timing in 99.3% of all cell-days. Our median uncertainty in the deconvolved burst onset time (σ_o) was 10.9 ± 6.4 ms (n=1,872 bursts), or approximately 1–2% of the duration of the song motif, reinforcing the notion that we could effectively monitor day-to-day activity changes within our network.

Our first step was to determine whether the number of spiking events changed over time. In the vast majority of our deconvolved neurons (321 out of 333, 96.4%), the burst number remained stable across observations (4.5±2.9 sessions spanning a range of 12.0 ± 7.4 days). Of the 12 cells that varied their burst number (Figure S1), four of these cases involved the complete elimination of spiking activity over time, transforming the neuron into a ‘silent’ cell that was no longer active during singing (Epsztein et al., 2011; Long et al., 2010). The remaining neurons exhibited changing burst numbers that switched between single and multiple bursts. Because it had been previously demonstrated that $HVC_{(RA)}$ neurons are only capable of producing a single burst during the song, while $HVC_{(X)}$ neurons can burst multiple times, these neurons likely belong to the latter category (Kozhevnikov and Fee, 2007) (Figure S1B).

We next determined whether the timing of neural activity in our recorded projection neurons shifted across observation sessions. We compared the estimated burst onset times of both single bursting (n = 246, e.g., Figure 2A) and multiple bursting (n = 87, e.g., Figure 2B) cells across many days. We focused first on an individual bird (Bird #102) from which we recorded 35 neurons (41 burst events) for more than two weeks (32.0 ± 10.4 days later). We plotted the results from the first and last imaging sessions for each cell (Figure 2C) and observed that the relative position of HVC bursting events remained consistent across time (Figure 2D), suggesting that sequential activity within HVC is surprisingly invariant in the adult zebra finch. To quantify the stability of all individual burst times, we next inspected the timing of song-related activity of the entire data set (Figure S2), and consistent timing across sessions was clearly evident for each burst event (Figure 2E).

Quantification of Network Stability

We then quantified the extent to which the timing of individual neurons was altered across observations by defining a 'distance score' for each burst, based on the absolute differences in onset times on individual days relative to the median onset time normalized by their joint standard deviations (Figure S3). In only 32 out of 1,869 cases (1.7%) was the distance score was greater than 3 (Figure 2E). These variable burst times were not biased towards any particular part of the song, either in their original time or their final time ($p>0.5$, KS test for uniformity). To examine the temporal distribution for individual bursts, we centered observations for each day around their median values (Figure 3A). We found tightly clustered time points across observations with a median standard deviation of 13.4 ms and a median range of 30.4 ms, a small fraction of the duration of the total song motif length (1.5 % and 3.5%, respectively) (Figure 3B). Because our ability to determine onset times varied widely across burst events, we reanalyzed our data, focusing on our most confident estimates ($\sigma_o < 10$ ms, 44% of burst events). These cases exhibited an even greater degree of stability (median standard deviation: 6.2 ms, median range: 12.4 ms), further confirming the invariant nature of the HVC network sequence.

We next asked if the small number of changes we observed in HVC burst timing could reflect a consistent drift within the network that is evolving over time, albeit at a slower pace than reported previously (Liberti et al., 2016). If this were true, we would expect to see that the timing of the network was slowly changing from baseline. Alternatively, changes in single neurons may simply represent temporary deviations and the overall timing of the network should remain consistent across observations. When we compared all bursts to the time of their first observation, we found no relationship between the magnitude of deviations and the observation date ($p > 0.5$, F-test) (Figure 3C), suggesting that any changes represented transient deviations from a stable representation.

One concern with these analyses is that inherent limitations in the temporal resolution of calcium imaging could prevent us from detecting changes in burst timing, leading to false negatives. To control for this possibility, we performed a progressive shuffling of our data, beginning with the cases where the burst timing within a session most significantly deviates from their median value across all sessions and gradually replacing all burst times. After each step, we recalculated the distance scores and asked whether this new shuffled

distribution differed from the original (Figure 3D). For this analysis we only analyzed pairwise distances across dates, avoiding the assumption that there is any “true” burst time (Figure S3). If the network were highly variable over time or our uncertainty limited our ability to detect changes, then replacing these bursts would minimally affect our distribution; we would expect that a large percentage of neurons would have to be replaced in order to see a difference between our original and our shuffled data sets. However, if our network were stable across time, then replacing only a small percentage of our most shifted neurons should lead to a statistically significant difference. Indeed, by only replacing 4.1% (one-tailed KS test, $p<0.05$) of our data points, we were able to detect a difference (Figure 3E), strongly supporting our claim that the network remains stable over time.

DISCUSSION

In this study, we used longitudinal imaging to analyze network dynamics in the absence of motor variability by examining the courtship song of the zebra finch. Birdsong has the distinct advantage of being both highly complex, with time-varying structure on a 10 ms timescale, as well as rigidly stereotyped, which facilitates longitudinal study. We found that a precisely executed motor behavior (i.e., directed singing in the zebra finch) is mediated by a set of highly stable component neurons, even over the period of several weeks. Our finding is notable because changes in the activity of premotor neurons were rarely observed, even though the precise activity inherent to HVC projection neurons (Hahnloser et al., 2002; Kozhevnikov and Fee, 2007) allows for the detection of differences on the scale of only a few milliseconds. Our results indicate that the HVC premotor network in the adult zebra finch appears to converge on a single solution for representing the song (tuning constancy hypothesis), rather than freely moving around within a larger manifold, despite the high degree of redundancy in the system (i.e., approximately 200 active neurons at each time point during singing (Fee et al., 2004; Lynch et al., 2016; Picardo et al., 2016). Therefore, the invariant structure of the adult zebra finch courtship song (Lombardino and Nottebohm, 2000) is likely due to the stable song-related firing activity of individual neurons within HVC.

Strikingly, the widespread stability observed here appears to contradict a recent report that used head-mounted 1-photon microscopes to demonstrate that ~40% of HVC projection neurons changed their activity across the span of only five days (Liberti et al., 2016) despite a low degree of variance within the behavior itself. However, the single photon imaging modality used in that study integrates signals from labeled neurons at depths ranging up to hundreds of microns (Helmchen and Denk, 2005), especially along the optical axis, due to the light scattering properties of neural tissue (Yaroslavsky et al., 2002). As a result, different neurons (with different responses during singing) are likely to have been included the same ROI (Zhou et al., 2018), leading to the illusion of instability at the single neuron level. Furthermore, the limited depth afforded by 1-photon imaging could make it difficult to distinguish whether a neuron is changing its activity or simply disappearing from view. Indeed, 68% of neurons in that study were not visible throughout the 5-day imaging period, strongly suggesting changes in the position of the microscope relative to the imaged tissue. Importantly, these issues are compounded when applied to HVC, which features small (7–10 μm) neurons often occurring in clumps and surrounded by heavily myelinated neuropil

(Burd and Nottebohm, 1985; Kirn et al., 1999). In contrast, our study used two-photon microscopy, whose optical sectioning abilities restricted our signal source to a single focal plane (Denk et al., 1990). We also leveraged this axial resolution to perform a careful and quantitative anatomical analysis on our optically sectioned tissue (Figures 1C–E), while *in vivo* single-photon head-mounted microscopes are not capable of such an exquisite anatomical analysis (Ghosh et al., 2011; Sheintuch et al., 2017).

Another potentially important difference between this set of experiments and the aforementioned HVC longitudinal imaging study is song context. In our study, zebra finches directed their singing behavior towards a female, whereas the birds in the previous report sang spontaneous (or undirected) song. Behaviorally, undirected song has been shown to exhibit significantly greater variance in both temporal and spectral properties compared with directed song (Sossinka and Bohner, 1980). Several lines of evidence have demonstrated that such variability arises from the anterior forebrain pathway (AFP) (Bottjer et al., 1984; Kao and Brainard, 2006; Olveczky et al., 2005), which is capable of influencing both downstream motor targets (Olveczky et al., 2011; Perkel, 2004) as well as specific aspects of song timing and syntax that are primarily thought to be mediated by HVC (Ali et al., 2013; Kao and Brainard, 2006; Thompson et al., 2011). Although HVC projection neuron activity during singing does not appear to exhibit context-dependent differences in neural responses within the span of an electrophysiological recording (~ 1 hour) (Woolley et al., 2014), future experiments should test for the possibility of slow network changes accompanying undirected singing using imaging methods similar to those presented here.

A number of other, more minor experimental differences also exist between our study and that previous work, and these are unlikely to have led to our contrasting conclusions. First, in our study the birds sang while head-fixed, whereas the previous study was performed in freely moving birds. Head-fixation has been demonstrated to eliminate sensory inputs that are crucial for some neural computations, such as the formation of place cells in a virtual environment (Ravassard et al., 2013). Regardless, we have recently tested the hypothesis that sensory information is affecting HVC premotor dynamics (Vallentin and Long, 2015) by systematically removing three sensory feedback streams (auditory, proprioceptive, and vagal). Such manipulations did not alter the frequency or temporal precision of song-related synaptic activity, suggesting that the sensory input does not affect HVC during song performance in the adult zebra finch. Additionally, birds perform only a small portion of the total amount of their daily songs while-head fixed, making it extremely unlikely that the dynamics underlying head-fixed song have diverged from those occurring during free movement. Consistent with this idea, we had previously shown that the song produced in a head-fixed configuration is acoustically indistinguishable from freely-moving song (Picardo et al., 2016). Second, our virus (Adeno-associated virus) differs from that used in the previous study (lentivirus), raising the possibility that different neurons may be infected in each case. However, each viral type has been shown to label significant numbers of both major HVC projection populations ($HVC_{(RA)}$ and $HVC_{(X)}$) (Liberti et al., 2016; Markowitz et al., 2015; Picardo et al., 2016).

Our results show that a premotor circuit tasked with generating a crystallized behavior can stabilize its network over long periods of time. Future work will establish whether the

dynamics observed in the zebra finch may represent a unique case or a more broadly applicable rule that is consistent across other model systems in which a stable behavior is required (Chestek et al., 2011; Flint et al., 2016; Fraser and Schwartz, 2012; Ganguly and Carmena, 2009). In contrast, other networks crucial for encoding new information may exhibit a higher degree of flexibility. For instance, in a recently published report (Driscoll et al., 2017), neurons in the parietal cortex of mice showed continuous changes in their tuning over days despite maintaining a stable representation at the level of the population, consistent with the optimal manifold hypothesis. Within the songbird model system, the observation of a stable song production network in the adult contrasts starkly with the highly dynamic network activity within HVC observed in juveniles during song acquisition (Adret et al., 2012; Crandall et al., 2007; Okubo et al., 2015; Vallentin et al., 2016). Furthermore, significant changes in singing behavior have been noted in the adult songbird following manipulations of auditory feedback (Konishi, 1965; Leonardo and Konishi, 1999; Tumer and Brainard, 2007). Such perturbations can change HVC connections (Tschida and Mooney, 2012) as well as song-related activity (Ali et al., 2013), but how these changes manifest at the network level remains unknown. The possibility exists that neurons maintain the capability of retuning following such large-scale manipulations, which may allow the network to compensate in order to influence behavioral performance (Otchy et al., 2015; Stauffer et al., 2012). In our study, the small number of cells that exhibited retuning may represent a subpopulation of malleable HVC neurons in the adult brain (e.g., Figure S1), potentially newly born projection cells within HVC (Paton and Nottebohm, 1984) or another dedicated set of neurons capable of changing their activity within an otherwise deterministic network (Rose et al., 2016).

Overall our results make a compelling case that the premotor network underlying singing behavior is mediated by a finely-tuned population of neurons with dynamics that can remain stable at long timescales. The circuit mechanisms underlying the long-term stability of this network remain elusive (Marder and Goaillard, 2006; Turrigiano, 2012). One possibility is that the bird actively reduces motor variability on a song-to-song basis by converging towards a similar neuronal state before initiating each song (Churchland et al., 2010; Rajan and Doupe, 2013). Additionally, mechanisms of circuit maintenance may also be in place to ensure consistency across longer timescales. For instance, in a previous study, we described changes in HVC inhibitory networks that help to decouple HVC from auditory inputs once a song is learned (Vallentin et al., 2016), potentially preventing external synaptic inputs from altering intrinsic circuitry. As a result, the HVC premotor network remains silent when the bird is not vocalizing (Hahnloser et al., 2002; Kozhevnikov and Fee, 2007), which could help to avoid synaptic changes that might arise from spike-timing dependent mechanisms (Feldman, 2012). In stark contrast, during song they produce high frequency bursts that are likely mediated by calcium spikes (Larkum et al., 2001), which have been shown to stabilize the generation of network sequences (Long et al., 2010) and may reinforce synaptic weights over time (Cichon and Gan, 2015).

STAR★METHODS

Detailed methods are provided in the online version of this paper and include the following:

CONTACT FOR REAGENTS AND RESOURCE SHARING

Further information and requests for resources and reagents should be directed to and will be fulfilled by the Lead Contact, Michael Long (mlong@med.nyu.edu).

EXPERIMENTAL MODEL AND SUBJECT DETAILS

Animals—Zebra finches were obtained from an outside breeder and maintained in a temperature and humidity controlled environment with a daily 12:12 light-dark schedule. All birds imaged in this study were adult males that were at least 90 days posthatch. Female zebra finches were used to elicit song. Animal maintenance and experimental procedures were performed according to the guidelines established by the Institutional Animal Care and Use Committee at the New York University Langone Medical Center.

Head-fixed singing preparation—Details concerning surgical implantation, behavioral training, and *in vivo* calcium imaging have been described elsewhere (Picardo et al., 2016). Briefly, a small headplate was implanted at the beginning of training to stabilize the skull. Detected song bouts (RPvdsEx and RX8, Tucker-Davis Technologies) were rewarded with 20 μl water droplets to encourage singing. Once the behavior was learned, a viral vector was introduced and the cranial window was implanted above HVC. We injected either AAV9.Syn.GCaMP6s.WPRE.SV40 (Penn Vector Core) or a 1:1 mix of AAV9.CamKII0.4.Cre.SV40 and either AAV9.CAG.Flex.GCaMP6f.WPRE.SV40 or AAV9.CAG.Flex.GCaMP6s.WPRE.SV40. We then used a customized Movable Objective Microscope (Sutter Instrument Company) and a resonant system (Thorlabs) to scan our field of view at 28.8 Hz ScanImage 4.2 software (Picardo et al., 2016). Imaging was done using a 16x water immersion objective (Nikon, MRP-07220) with a numerical aperture of 0.8 and a working distance of 3 mm. All experiments were performed between 1.5 and 2.5 hours after the lights turned on in the morning. Frames captured during singing behavior were aligned to a canonical song via linear temporal warping for further analysis.

METHOD DETAILS

Image Analysis—To obtain the song-related fluorescence traces of individual neurons, images within and across motifs were motion corrected (Miri et al., 2011), and cells were manually outlined (ImageJ) on the average of each plane. Fluorescence traces were extracted by taking the mean pixel value within the respective ROIs. The presence of song-related activity was confirmed by visual inspection by up to three different individuals within the laboratory using a GUI designed to randomly present the activity of individual neurons for confirmation.

We next split the plane's average image into individual days. For each day, all cells were inspected to visually confirm that they were successfully captured. If a cell was not seen in the proper location on a specific day, then its data for that day were removed from further analysis. We compared the local neighborhood of all cell-days across time by assigning spatial scores in which the similarity for each pair of cell-days was computed by removing the pixels within both ROIs and performing a 2D correlation on the remaining pixels. If a cell was acquired at the edge of the frame on any given day, precluding analysis of the entire 100 μm neighborhood, then only the area imaged on both days was used for comparison.

The spatial correlation score for each cell-day was defined as the median of correlations with other cell-days within the same cell. Cell-days with a spatial correlation score below the upper bound of the 98th percentile of the null distribution (i.e., cell-days across cells) were removed from further analysis. Unless otherwise noted, all data analyses were performed using custom MATLAB scripts (Mathworks).

Burst Deconvolution—Burst onset times were estimated from the song-aligned fluorescence traces using the Markov Chain-Monte Carlo (MCMC) inference method described previously (Picardo et al., 2016; Pnevmatikakis et al., 2016). In contrast to our previous analytical approach (Picardo et al., 2016), we considered each cell-day independently of all other days within that cell. We modeled the fluorescence traces as a sum of double exponentials placed at each burst time. The onsets and time constants of bursts were assumed to be consistent across trials within a single cell-day, though baselines, burst amplitudes, and noise statistics were allowed to be unique for individual motifs. To efficiently explore the parameter space, we used MCMC to approximate the posterior distributions of each parameter individually by probabilistically generating samples from them in a stepwise manner. Each sweep of the sampler proposed a change to each parameter individually, such as the number of bursts or the baseline amplitudes. Early sweeps (the first 1500) were removed from analysis. We initialized the MCMC sampler to the same state for all cell-days. In some cases, this approach sometime led to a failure to converge at an appropriate solution, and specific information concerning the cell-day could be provided to avoid local minima. For instance, a large deviation in a fluorescence trace could sometimes be mistaken for two closely spaced events. To counteract this, the minimum distance between bursts (two sampling bins, or roughly 70 ms) was enforced for those trials. Initial burst times were either assigned before the onset of song or at a randomly shifted location within the song motif. Cell-days that did not converge to appropriate solutions after additional information was provided were removed from further analysis to prevent bias. To extract the estimated burst onset times, we fit a Gaussian mixture distribution initialized on the peaks of the histogram of their posterior distribution. Clustering errors were corrected manually. Burst onsets for each cell were then defined as the medians of the posterior of the respective subsets. For these measures as well as any other descriptive statistics whose underlying distribution is not normal, we present the median value with uncertainty defined as 1.48 times the median absolute deviation.

QUANTIFICATION AND STATISTICAL ANALYSIS

Calculating Changes in Neuronal Representation of Song—We evaluated the stability of activity of individual neurons during singing across days using two primary metrics. First, we compared the number of burst events for each cell-day relative to the modal number of burst events observed across all days. Next, the timing of each burst event within a cell was compared to the median burst time across of its observations. If there was more than one burst on any day, we calculated all pairwise distances between each burst on each set of days and assigned closest pairs until all bursts were assigned or only one burst remained using a greedy matching algorithm that minimized pairwise distances with burst times within that cell on all other days. We took a bootstrapping approach to define our median burst time in order to incorporate our uncertainty across days. For each iteration

(n=1,000), all burst times were shifted by a random number drawn from a gaussian distribution scaled by their respective uncertainty and the median of these times was calculated. The median time and uncertainty was then defined as the mean and standard deviation of these times. Temporal distances between individual bursts and the median time were normalized by their joint standard deviation ($\sigma=\sqrt{(\sigma_i^2 + \sigma_{true}^2)}$ for each day i) to create a distance score for each burst.

We next formally tested the hypothesis that our uncertainty in burst timing estimation did not impact our ability to detect timing changes by parametrically shuffling burst times and comparing the distributions of the new distance scores with our true data. For each cell, new burst times were sampled with replacement from the distribution of all other burst times observed in that bird. We smoothly interpolated across the percentage of bursts (bootstrapping, n=100 for each 0.1 percent) that were changed, beginning with the bursts that already had the highest distance scores. For this process, burst variances were not changed, nor were the number of bursts. Since there was no longer a true burst time, distance scores here were defined as the median pairwise distance scores. A one-tailed Kolgorov-Smirnov test was used on each new distribution of distance scores, comparing the CDF generated from purposefully changing burst times with that of the real data. The point at which we could statistically distinguish between these distributions and true data reflected an upper threshold on the percentage of the network that changed over our observation period.

DATA AND SOFTWARE AVAILABILITY

The data that support the findings of this study are available from the corresponding author upon reasonable request.

KEY RESOURCES TABLE

REAGENT or RESOURCE	SOURCE	IDENTIFIER
Bacterial and Virus Strains		
AAV9.Syn.GCaMP6s.WPRE.SV40	Penn Vector Core	N/A
AAV9.CamKII0.4.Cre.SV40	Penn Vector Core	N/A
AAV9.CAG.Flex.GCaMP6f.WPRE.SV40	Penn Vector Core	N/A
AAV9.CAG.Flex.GCaMP6s.WPRE.SV40	Penn Vector Core	N/A
Experimental Models: Organisms/Strains		
Zebra Finch (*Taeniopygia guttata*)	Magnolia Bird Farms, Anaheim CA	N/A
Software and Algorithms		
MATLAB	Mathworks	https://www.mathworks.com/products/matlab.html
ImageJ	NIH	https://imagej.nih.gov/ij/
Markov Chain Monte Carlo deconvolution	Picardo et al. 2016	https://doi.org/10.1016/j.neuron.2016.02.016
RPvdsEx	Tucker-Davis Technologies	http://www.tdt.com/rpvdsex.html
ScanImage	Vidrio Technologies	ScanImage 4.2 (2015)

REAGENT or RESOURCE	SOURCE	IDENTIFIER
Other		
Digital Signal Processor	Tucker-Davis Technologies	RX8
Resonant Scanner	Thorlabs	N/A
Movable Objective Microscope	Sutter Instrument Company	N/A
16x Water Immersion Objective	Nikon	MRP-07220

Supplementary Material

Refer to Web version on PubMed Central for supplementary material.

Acknowledgments

This research was supported by the NIH (R01NS075044, TR001447), the New York Stem Cell Foundation, the Rita Allen Foundation, Simons Foundation (Global Brain Initiative), and EMBO (ALTF 1608-2013). We thank Aimee Chow, Rachel Clary, and Madeleine Junkins for their technical assistance. We thank members of the Long laboratory, Kishore Kuchibhotla, Dmitriy Aronov for comments on an earlier draft of this manuscript as well as Jeff Gauthier, Peyman Golshani, and Daniel Dombeck for helpful discussions. We acknowledge the GENIE Program and the Janelia Farm Research Campus, specifically Vivek Jayaraman, Ph.D., Rex A. Kerr, Ph.D., Douglas S. Kim, Ph.D., Loren L. Looger, Ph.D., Karel Svoboda, Ph.D. from the GENIE Project, Janelia Farm Research Campus, Howard Hughes Medical Institute.

References

Adret P, Meliza CD, Margoliash D. Song tutoring in presinging zebra finch juveniles biases a small population of higher-order song-selective neurons toward the tutor song. J Neurophysiol. 2012; 108:1977–1987. [PubMed: 22786956]

Ali F, Otchy TM, Pehlevan C, Fantana AL, Burak Y, Olveczky BP. The basal ganglia is necessary for learning spectral, but not temporal, features of birdsong. Neuron. 2013; 80:494–506. [PubMed: 24075977]

Bottjer SW, Miesner EA, Arnold AP. Forebrain lesions disrupt development but not maintenance of song in passerine birds. Science. 1984; 224:901–903. [PubMed: 6719123]

Burd GD, Nottebohm F. Ultrastructural characterization of synaptic terminals formed on newly generated neurons in a song control nucleus of the adult canary forebrain. J Comp Neurol. 1985; 240:143–152. [PubMed: 4056107]

Carmena JM, Lebedev MA, Henriquez CS, Nicolelis MA. Stable ensemble performance with single-neuron variability during reaching movements in primates. J Neurosci. 2005; 25:10712–10716. [PubMed: 16291944]

Chaisanguanthum KS, Shen HH, Sabes PN. Motor variability arises from a slow random walk in neural state. J Neurosci. 2014; 34:12071–12080. [PubMed: 25186752]

Chestek CA, Gilja V, Nuyujukian P, Foster JD, Fan JM, Kaufman MT, Churchland MM, Rivera-Alvidrez Z, Cunningham JP, Ryu SI, et al. Long-term stability of neural prosthetic control signals from silicon cortical arrays in rhesus macaque motor cortex. J Neural Eng. 2011; 8:045005. [PubMed: 21775782]

Churchland MM. Using the precision of the primate to study the origins of movement variability. Neuroscience. 2015; 296:92–100. [PubMed: 25595983]

Churchland MM, Cunningham JP, Kaufman MT, Ryu SI, Shenoy KV. Cortical preparatory activity: representation of movement or first cog in a dynamical machine? Neuron. 2010; 68:387–400. [PubMed: 21040842]

Cichon J, Gan WB. Branch-specific dendritic Ca(2+) spikes cause persistent synaptic plasticity. Nature. 2015; 520:180–185. [PubMed: 25822789]

Clopath C, Bonhoeffer T, Hubener M, Rose T. Variance and invariance of neuronal long-term representations. Philos Trans R Soc Lond B Biol Sci. 2017; 372

Crandall SR, Adam M, Kinnischtzke AK, Nick TA. HVC neural sleep activity increases with development and parallels nightly changes in song behavior. J Neurophysiol. 2007; 98:232–240. [PubMed: 17428907]

Crowe SE, Ellis-Davies GC. Longitudinal in vivo two-photon fluorescence imaging. J Comp Neurol. 2014; 522:1708–1727. [PubMed: 24214350]

Denk W, Strickler JH, Webb WW. Two-photon laser scanning fluorescence microscopy. Science. 1990; 248:73–76. [PubMed: 2321027]

Driscoll LN, Pettit NL, Minderer M, Chettih SN, Harvey CD. Dynamic Reorganization of Neuronal Activity Patterns in Parietal Cortex. Cell. 2017; 170:986–999e916. [PubMed: 28823559]

Dutar P, Vu HM, Perkel DJ. Multiple cell types distinguished by physiological, pharmacological, and anatomic properties in nucleus HVc of the adult zebra finch. J Neurophysiol. 1998; 80:1828–1838. [PubMed: 9772242]

Epsztein J, Brecht M, Lee AK. Intracellular determinants of hippocampal CA1 place and silent cell activity in a novel environment. Neuron. 2011; 70:109–120. [PubMed: 21482360]

Fee MS, Kozhevnikov AA, Hahnloser RH. Neural mechanisms of vocal sequence generation in the songbird. Ann N Y Acad Sci. 2004; 1016:153–170. [PubMed: 15313774]

Feldman DE. The spike-timing dependence of plasticity. Neuron. 2012; 75:556–571. [PubMed: 22920249]

Flint RD, Scheid MR, Wright ZA, Solla SA, Slutzky MW. Long-Term Stability of Motor Cortical Activity: Implications for Brain Machine Interfaces and Optimal Feedback Control. J Neurosci. 2016; 36:3623–3632. [PubMed: 27013690]

Fraser GW, Schwartz AB. Recording from the same neurons chronically in motor cortex. J Neurophysiol. 2012; 107:1970–1978. [PubMed: 22190623]

Gallego JA, Perich MG, Miller LE, Solla SA. Neural Manifolds for the Control of Movement. Neuron. 2017; 94:978–984. [PubMed: 28595054]

Ganguly K, Carmena JM. Emergence of a stable cortical map for neuroprosthetic control. PLoS Biol. 2009; 7:e1000153. [PubMed: 19621062]

Ghosh KK, Burns LD, Cocker ED, Nimmerjahn A, Ziv Y, Gamal AE, Schnitzer MJ. Miniaturized integration of a fluorescence microscope. Nat Methods. 2011; 8:871–878. [PubMed: 21909102]

Glaze CM, Troyer TW. Temporal structure in zebra finch song: implications for motor coding. J Neurosci. 2006; 26:991–1005. [PubMed: 16421319]

Goller F, Cooper BG. Peripheral motor dynamics of song production in the zebra finch. Ann N Y Acad Sci. 2004; 1016:130–152. [PubMed: 15313773]

Graber MH, Helmchen F, Hahnloser RH. Activity in a premotor cortical nucleus of zebra finches is locally organized and exhibits auditory selectivity in neurons but not in glia. PLoS One. 2013; 8:e81177. [PubMed: 24312533]

Hahnloser RH, Kozhevnikov AA, Fee MS. An ultra-sparse code underlies the generation of neural sequences in a songbird. Nature. 2002; 419:65–70. [PubMed: 12214232]

Helmchen F, Denk W. Deep tissue two-photon microscopy. Nat Methods. 2005; 2:932–940. [PubMed: 16299478]

Hore J, Watts S. Skilled throwers use physics to time ball release to the nearest millisecond. J Neurophysiol. 2011; 106:2024–2033. [PubMed: 21775713]

Huber D, Gutnisky DA, Peron S, O'Connor DH, Wiegert JS, Tian L, Oertner TG, Looger LL, Svoboda K. Multiple dynamic representations in the motor cortex during sensorimotor learning. Nature. 2012; 484:473–478. [PubMed: 22538608]

Immelmann K. Song development in the zebra finch and other estrildid finches. In: Hinde RA, editorBird Vocalizations. London: Cambridge University Press; 1969. 61–74.

Kao MH, Brainard MS. Lesions of an avian basal ganglia circuit prevent context-dependent changes to song variability. J Neurophysiol. 2006; 96:1441–1455. [PubMed: 16723412]

Kawai R, Markman T, Poddar R, Ko R, Fantana AL, Dhawale AK, Kampff AR, Olveczky BP. Motor cortex is required for learning but not for executing a motor skill. Neuron. 2015; 86:800–812. [PubMed: 25892304]

Kirn JR, Fishman Y, Sasportas K, Alvarez-Buylla A, Nottebohm F. Fate of new neurons in adult canary high vocal center during the first 30 days after their formation. J Comp Neurol. 1999; 411:487–494. [PubMed: 10413781]

Konishi M. Effects of deafening on song development in American robins and black-headed grosbeaks. Z Tierpsychol. 1965; 22:584–599. [PubMed: 5879978]

Kozhevnikov AA, Fee MS. Singing-related activity of identified HVC neurons in the zebra finch. J Neurophysiol. 2007; 97:4271–4283. [PubMed: 17182906]

Larkum ME, Zhu JJ, Sakmann B. Dendritic mechanisms underlying the coupling of the dendritic with the axonal action potential initiation zone of adult rat layer 5 pyramidal neurons. J Physiol. 2001; 533:447–466. [PubMed: 11389204]

Lashley KS. Integrative functions of the cerebral cortex. Physiol Rev. 1933; 13:1–43.

Latash ML. The bliss (not the problem) of motor abundance (not redundancy). Exp Brain Res. 2012; 217:1–5. [PubMed: 22246105]

Leonardo A, Konishi M. Decrystallization of adult birdsong by perturbation of auditory feedback. Nature. 1999; 399:466–470. [PubMed: 10365958]

Liberti WA 3rd, Markowitz JE, Perkins LN, Liberti DC, Leman DP, Guitchounts G, Velho T, Kotton DN, Lois C, Gardner TJ. Unstable neurons underlie a stable learned behavior. Nat Neurosci. 2016; 19:1665–1671. [PubMed: 27723744]

Lombardino AJ, Nottebohm F. Age at deafening affects the stability of learned song in adult male zebra finches. J Neurosci. 2000; 20:5054–5064. [PubMed: 10864963]

Long MA, Fee MS. Using temperature to analyse temporal dynamics in the songbird motor pathway. Nature. 2008; 456:189–194. [PubMed: 19005546]

Long MA, Jin DZ, Fee MS. Support for a synaptic chain model of neuronal sequence generation. Nature. 2010; 468:394–399. [PubMed: 20972420]

Lutcke H, Margolis DJ, Helmchen F. Steady or changing? Long-term monitoring of neuronal population activity. Trends Neurosci. 2013; 36:375–384. [PubMed: 23608298]

Lynch GF, Okubo TS, Hanuschkin A, Hahnloser RH, Fee MS. Rhythmic Continuous-Time Coding in the Songbird Analog of Vocal Motor Cortex. Neuron. 2016; 90:877–892. [PubMed: 27196977]

Marder E, Goaillard JM. Variability, compensation and homeostasis in neuron and network function. Nat Rev Neurosci. 2006; 7:563–574. [PubMed: 16791145]

Marder E, Goeritz ML, Otopalik AG. Robust circuit rhythms in small circuits arise from variable circuit components and mechanisms. Curr Opin Neurobiol. 2015; 31:156–163. [PubMed: 25460072]

Markowitz JE, Liberti WA 3rd, Guitchounts G, Velho T, Lois C, Gardner TJ. Mesoscopic patterns of neural activity support songbird cortical sequences. PLoS Biol. 2015; 13:e1002158. [PubMed: 26039895]

Miri A, Daie K, Arrenberg AB, Baier H, Aksay E, Tank DW. Spatial gradients and multidimensional dynamics in a neural integrator circuit. Nat Neurosci. 2011; 14:1150–1159. [PubMed: 21857656]

Mooney R. Different subthreshold mechanisms underlie song selectivity in identified HVc neurons of the zebra finch. J Neurosci. 2000; 20:5420–5436. [PubMed: 10884326]

Moore GP, Chen J. Timings and interactions of skilled musicians. Biol Cybern. 2010; 103:401–414. [PubMed: 21046143]

Muceli S, Falla D, Farina D. Reorganization of muscle synergies during multidirectional reaching in the horizontal plane with experimental muscle pain. J Neurophysiol. 2014; 111:1615–1630. [PubMed: 24453279]

Narayanan NS, Kimchi EY, Laubach M. Redundancy and synergy of neuronal ensembles in motor cortex. J Neurosci. 2005; 25:4207–4216. [PubMed: 15858046]

Nasu D, Matsuo T, Kadota K. Two types of motor strategy for accurate dart throwing. PLoS One. 2014; 9:e88536. [PubMed: 24533102]

Nottebohm F, Stokes TM, Leonard CM. Central control of song in the canary, Serinus canarius. J Comp Neurol. 1976; 165:457–486. [PubMed: 1262540]

Okubo TS, Mackevicius EL, Payne HL, Lynch GF, Fee MS. Growth and splitting of neural sequences in songbird vocal development. Nature. 2015; 528:352–357. [PubMed: 26618871]

Olveczky BP, Andalman AS, Fee MS. Vocal experimentation in the juvenile songbird requires a basal ganglia circuit. PLoS Biol. 2005; 3:e153. [PubMed: 15826219]

Olveczky BP, Otchy TM, Goldberg JH, Aronov D, Fee MS. Changes in the neural control of a complex motor sequence during learning. J Neurophysiol. 2011; 106:386–397. [PubMed: 21543758]

Orban G, Wolpert DM. Representations of uncertainty in sensorimotor control. Curr Opin Neurobiol. 2011; 21:629–635. [PubMed: 21689923]

Otchy TM, Wolff SB, Rhee JY, Pehlevan C, Kawai R, Kempf A, Gobes SM, Olveczky BP. Acute off-target effects of neural circuit manipulations. Nature. 2015; 528:358–363. [PubMed: 26649821]

Paton JA, Nottebohm FN. Neurons generated in the adult brain are recruited into functional circuits. Science. 1984; 225:1046–1048. [PubMed: 6474166]

Peh WY, Roberts TF, Mooney R. Imaging auditory representations of song and syllables in populations of sensorimotor neurons essential to vocal communication. J Neurosci. 2015; 35:5589–5605. [PubMed: 25855175]

Perkel DJ. Origin of the anterior forebrain pathway. Ann N Y Acad Sci. 2004; 1016:736–748. [PubMed: 15313803]

Peters AJ, Chen SX, Komiyama T. Emergence of reproducible spatiotemporal activity during motor learning. Nature. 2014; 510:263–267. [PubMed: 24805237]

Peters AJ, Lee J, Hedrick NG, O'Neil K, Komiyama T. Reorganization of corticospinal output during motor learning. Nat Neurosci. 2017; 20:1133–1141. [PubMed: 28671694]

Picardo MA, Merel J, Katlowitz KA, Vallentin D, Okobi DE, Benezra SE, Clary RC, Pnevmatikakis EA, Paninski L, Long MA. Population-Level Representation of a Temporal Sequence Underlying Song Production in the Zebra Finch. Neuron. 2016; 90:866–876. [PubMed: 27196976]

Pnevmatikakis EA, Soudry D, Gao Y, Machado TA, Merel J, Pfau D, Reardon T, Mu Y, Lacefield C, Yang W, et al. Simultaneous Denoising, Deconvolution, and Demixing of Calcium Imaging Data. Neuron. 2016; 89:285–299. [PubMed: 26774160]

Rajan R, Doupe AJ. Behavioral and neural signatures of readiness to initiate a learned motor sequence. Curr Biol. 2013; 23:87–93. [PubMed: 23246408]

Ravassard P, Kees A, Willers B, Ho D, Aharoni DA, Cushman J, Aghajan ZM, Mehta MR. Multisensory control of hippocampal spatiotemporal selectivity. Science. 2013; 340:1342–1346. [PubMed: 23641063]

Rokni U, Richardson AG, Bizzi E, Seung HS. Motor learning with unstable neural representations. Neuron. 2007; 54:653–666. [PubMed: 17521576]

Rose T, Jaepel J, Hubener M, Bonhoeffer T. Cell-specific restoration of stimulus preference after monocular deprivation in the visual cortex. Science. 2016; 352:1319–1322. [PubMed: 27284193]

Sheintuch L, Rubin A, Brande-Eilat N, Geva N, Sadeh N, Pinchasof O, Ziv Y. Tracking the Same Neurons across Multiple Days in Ca(2+) Imaging Data. Cell Rep. 2017; 21:1102–1115. [PubMed: 29069591]

Sossinka R, Bohner J. Song types of the zebra finch Poephila guttata castanotis. Z Tierpsychol. 1980; 53:123–132.

Stauffer TR, Elliott KC, Ross MT, Basista MJ, Hyson RL, Johnson F. Axial organization of a brain region that sequences a learned pattern of behavior. J Neurosci. 2012; 32:9312–9322. [PubMed: 22764238]

Takiyama K, Okada M. Maximization of learning speed in the motor cortex due to neuronal redundancy. PLoS Comput Biol. 2012; 8:e1002348. [PubMed: 22253586]

Tchernichovski O, Mitra PP, Lints T, Nottebohm F. Dynamics of the vocal imitation process: how a zebra finch learns its song. Science. 2001; 291:2564–2569. [PubMed: 11283361]

Thompson JA, Basista MJ, Wu W, Bertram R, Johnson F. Dual pre-motor contribution to songbird syllable variation. J Neurosci. 2011; 31:322–330. [PubMed: 21209218]

Todorov E, Jordan MI. Optimal feedback control as a theory of motor coordination. Nat Neurosci. 2002; 5:1226–1235. [PubMed: 12404008]

Tschida KA, Mooney R. Deafening drives cell-type-specific changes to dendritic spines in a sensorimotor nucleus important to learned vocalizations. Neuron. 2012; 73:1028–1039. [PubMed: 22405211]

Tumer EC, Brainard MS. Performance variability enables adaptive plasticity of 'crystallized' adult birdsong. Nature. 2007; 450:1240–1244. [PubMed: 18097411]

Turrigiano G. Homeostatic synaptic plasticity: local and global mechanisms for stabilizing neuronal function. Cold Spring Harb Perspect Biol. 2012; 4:a005736. [PubMed: 22086977]

Vallentin D, Kosche G, Lipkind D, Long MA. Neural circuits. Inhibition protects acquired song segments during vocal learning in zebra finches. Science. 2016; 351:267–271. [PubMed: 26816377]

Vallentin D, Long MA. Motor origin of precise synaptic inputs onto forebrain neurons driving a skilled behavior. J Neurosci. 2015; 35:299–307. [PubMed: 25568122]

Vu ET, Mazurek ME, Kuo YC. Identification of a forebrain motor programming network for the learned song of zebra finches. J Neurosci. 1994; 14:6924–6934. [PubMed: 7965088]

Wollner C, Deconinck FJ, Parkinson J, Hove MJ, Keller PE. The perception of prototypical motion: synchronization is enhanced with quantitatively morphed gestures of musical conductors. J Exp Psychol Hum Percept Perform. 2012; 38:1390–1403. [PubMed: 22506779]

Woolley SC, Rajan R, Joshua M, Doupe AJ. Emergence of context-dependent variability across a basal ganglia network. Neuron. 2014; 82:208–223. [PubMed: 24698276]

Yaroslavsky AN, Schulze PC, Yaroslavsky IV, Schober R, Ulrich F, Schwarzmaier HJ. Optical properties of selected native and coagulated human brain tissues in vitro in the visible and near infrared spectral range. Phys Med Biol. 2002; 47:2059–2073. [PubMed: 12118601]

Zhou P, Resendez SL, Rodriguez-Romaguera J, Jimenez JC, Neufeld SQ, Giovannucci A, Friedrich J, Pnevmatikakis EA, Stuber GD, Hen R, et al. Efficient and accurate extraction of in vivo calcium signals from microendoscopic video data. Elife. 2018; 7

Highlights

- Monitored the activity of individual neurons in a singing bird over several weeks
- The number and timing of song-related spiking events remained nearly identical
- Stability in motor behaviors can be achieved through invariant neuronal tuning

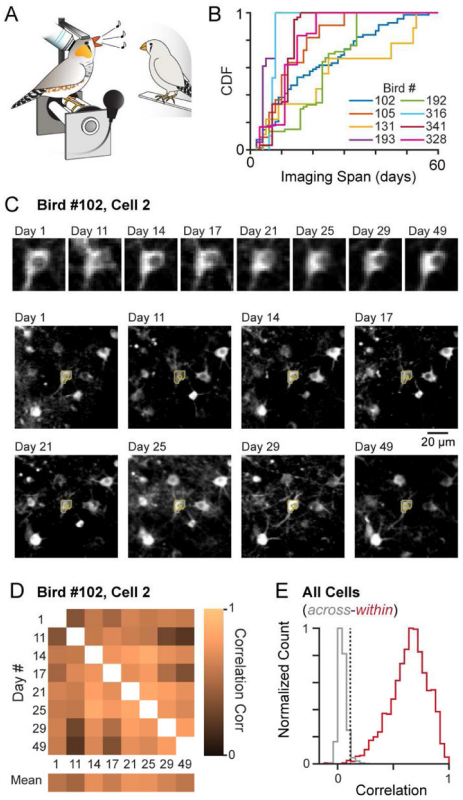

Figure 1. Longitudinal Imaging of HVC Song-related Network Activity

(A) Birds were trained in a head-fixed configuration, enabling two-photon microscopy during directed singing.

(B) Cumulative distributions for recording durations, defined as the elapsed time between the first and last imaging sessions for each neuron.

(C) Anatomical characterization of a representative neuron. For each cell in the study, the cell body (top) and the local region surrounding each neuron (bottom) were analyzed. Each image is an average across all song trials for a specific day. Yellow outline indicates the ROI.

(D) Spatial cross-correlations between local regions of an ROI on different days.

(E) Distributions of mean spatial scores within an ROI (red) compared with those across ROIs (grey). Cell-days with spatial scores below the upper 98% confidence interval of the null distribution (dashed line, r = 0.11) were removed.

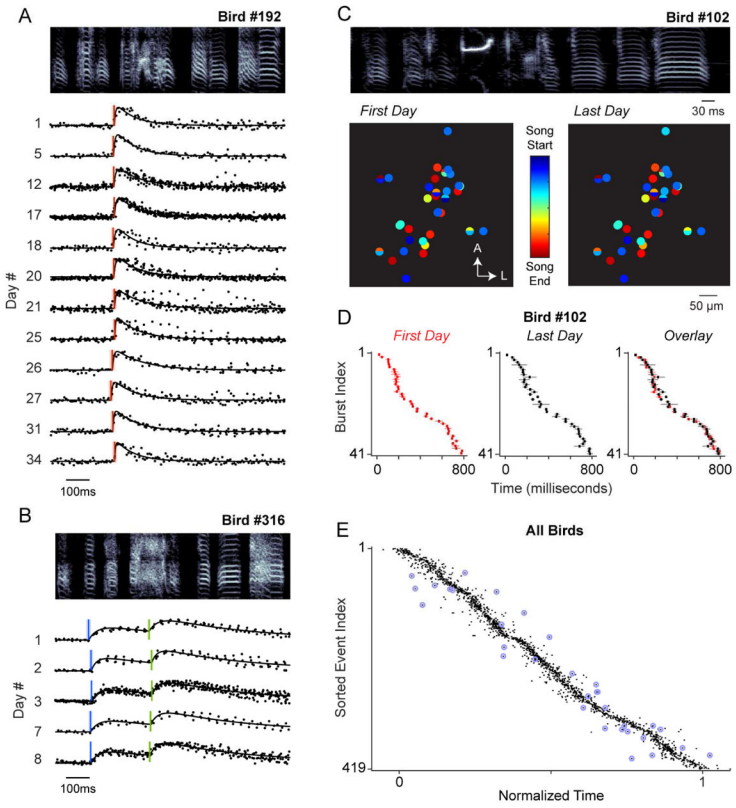

Figure 2. Song-related Neuronal Activity Within HVC is Stable Across Time

(A and B) An example of the longitudinal song-related activity from a single bursting (A) and a double bursting (B) cell in Birds #192 and #316, respectively. Representative sonograms provided for each bird. Fluorescence measurements normalized between pre-song average and peak fluorescence are shown across aligned trials from a single day (dots), and the average modeled fit is included as a black line (see Methods). Vertical lines indicate estimated burst times, with shading representing the uncertainty (± 2σ). See also Figure S1.

(C) At top, a representative sonogram for Bird #102. At bottom, 35 HVC projection neurons imaged for greater than two weeks following their initial observations. The position of each neuron is represented by a circle whose color indicates the time during the song motif when the neuron is active. Neurons with two bursts (n = 6) are split horizontally with the bottom and top colors corresponding to the onset times of the first and second burst events, respectively. See also Figure S2.

(D) Each burst event shown in (C), including the first observation, the last observation, and an overlay, with the vertical line in each row indicating the burst onset time and the width of horizontal lines signifying the uncertainty (± 2σ). Events are sorted based on the median time across all observations.

(E) All 419 unique burst events from 333 cells, normalized for song duration across different birds and sorted by the median event time across days. Individual tick marks represent independent observations across days. Divergent points defined by distance scores greater than 3 are circled in blue. See also Figure S3.

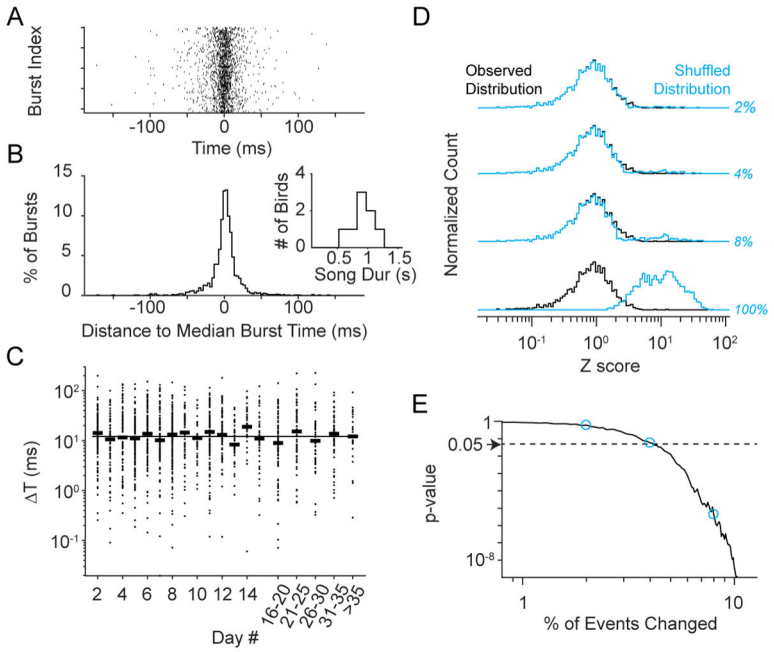

Figure 3. Quantification of Longitudinal Changes in HVC Burst Timing

(A) Observed bursts centered to their respective median times across all sessions. Events are vertically sorted based on their absolute timing relative to the song motif with earlier bursts represented at the top.

(B) Distribution of temporal distances to the median event time across all bursts. Inset: Distribution of song durations for all 8 birds.

(C) The change relative to the first day for all burst times as a function of observation date. Horizonal bars indicate the median for each day, and the line represents the median absolute change across all observations (12.1 ms).

(D) Comparison of four example distributions of distance scores from the shuffled data sets (blue) with the true distribution (black). Numbers at right indicate the percentage of bursts shuffled.

(E) Hypothesis testing on the observed versus shuffled distributions. Blue circles indicate p-values for the 2%, 4% and 8% shuffled cases, as shown in (C). Dashed line represents p = 0.05 (4.1% of the data set), below which we can statistically differentiate between the observed and shuffled data.